NeuroImage: Clinical 6 (2014) 237–242

Contents lists available at ScienceDirect

NeuroImage: Clinical

journal homepage: www.elsevier.com/locate/ynicl

Magnetization transfer ratio recovery in new lesions decreases during adolescence in pediatric-onset multiple sclerosis patients

Robert A. Brown[a,*], Sridar Narayanan[a], Brenda Banwell[b], Douglas L. Arnold[a], on behalf of the Canadian Pediatric Demyelinating Disease Network

[a]McConnell Brain Imaging Centre, Montreal Neurological Institute and Hospital 3801 Rue University, Montreal H3A 2B4, Canada
[b]Division of Neurology, Children's Hospital of Philadelphia, Philadelphia, USA

ARTICLE INFO

Article history:
Received 11 June 2014
Received in revised form 25 August 2014
Accepted 5 September 2014
Available online 10 September 2014

Keywords:
MRI
Multiple sclerosis
Remyelination
Pediatric multiple sclerosis

ABSTRACT

Children and adolescents diagnosed with multiple sclerosis rarely accrue physical disability early in their disease. This could be explained by greater remyelination in children, a capacity that may be lost in adolescence or early adulthood. Magnetization transfer ratio (MTR) MRI can be used to quantify changes in myelin in MS. We used serial MTR imaging and longitudinal random effects analysis to quantify recovery of MTR in acute lesions and to evaluate MTR changes in normal-appearing tissue in 19 adolescent MS patients. Our objective was to determine whether younger adolescents have a greater capacity for remyelination and whether this decreases as patients approach adulthood. We detected a significant decrease in MTR recovery between ages 16 and 20 years ($p = 0.023$), with older subjects approaching typical recovery levels for adult-onset MS. MTR recovery in acute MS lesions decreases with age in adolescents, suggesting loss of remyelination capacity. This may be related to the conclusion of primary myelination or other developmental factors.

1. Introduction

Multiple sclerosis (MS) is an autoimmune disease characterized by the formation of inflammatory demyelinating lesions in the central nervous system. Although MS is normally diagnosed in adults, some patients experience clinical onset before the age of 18 (Banwell et al., 2007).

Focal MS lesions vary in their degree of myelin loss. Histopathological analysis of remyelination in the brain of MS patients is limited, and most specimens have been obtained from older adults with long-standing and often secondary progressive MS. Fully demyelinated lesions are common in these patients (Miller et al., 1996), but partially remyelinated "shadow plaques" are also observed (Patrikios et al., 2006), indicating that the adult brain has some ability to repair myelin. It has been suggested that remyelination capacity decreases with age (Fancy et al., 2010; Franklin et al., 2002) in humans and in animal models of induced CNS demyelination (Hinks and Franklin, 2000; Ruckh et al., 2012; Shen et al., 2008; Sim et al., 2002).

If remyelination capacity decreases with age in adults, we would expect children and adolescents with MS to have an even greater capacity for remyelination, and some clinical features of pediatric-onset MS suggest that this may be true. Children and adolescents usually recover completely from their first attack (Bigi and Banwell, 2012; Ruggieri et al., 2004) and rarely accrue physical disability within the first 10 years of the disease (Renoux et al., 2007).

In order to investigate myelination as a function of age, as well as lesional remyelination capacity *in vivo*, an imaging technique sensitive to changes in myelin content is needed. Suitable methods include myelin water fraction (MWF), derived from multicomponent T2 mapping; restricted proton pool size, derived from quantitative magnetization transfer (qMT) imaging; and magnetization transfer ratio (MTR), which is a semi-quantitative measurement of magnetization exchange between free and bound proton pools. We have used an MTR-based approach in this study because data with the required resolution for lesion-based analyses can be acquired relatively quickly, an important issue for pediatric studies. MTR has been histopathologically validated as a marker for myelin in both humans and animals and has excellent quantitative correlation with the Luxol fast blue stain, which is attracted to lipoproteins in the myelin sheath and is used as a standard stain for myelin (Barkhof et al., 2003; Chen et al., 2007; Deloire-Grassin et al., 2000; Dousset et al., 1992; Pike et al., 2000; Schmierer et al., 2004).

* Corresponding author.
E-mail addresses: robert.brown@mcgill.ca (R.A. Brown), banwellb@email.chop.edu (B. Banwell), douglas.arnold@mcgill.ca (D.L. Arnold).

http://dx.doi.org/10.1016/j.nicl.2014.09.003

Changes in MTR over time in new lesions exhibit a typical pattern of sudden decrease at the time of lesion formation, followed by partial recovery. We have developed an MTR imaging-based technique that uses longitudinal scanning to identify focal areas of tissue that experience an acute decrease in MTR (corresponding to demyelination) and quantify subsequent recovery (remyelination) (Brown et al., 2012). These "ΔMTR" lesions are distinct from other lesion types normally identified in MS, such as hyperintensities on T2-weighted or gadolinium contrast enhanced scans; because they are identified on MTR images, they are more specific to demyelination (Brown et al., 2012). The MTR timecourse within these lesions can be modeled and produces a statistically powerful measurement of differences in MTR recovery, indicative of remyelination.

If the capacity for repair of MS lesions is particularly robust when concurrent with ongoing myelin maturation or other developmental factors, we would expect that adolescent MS patients would have a greater capacity to repair lesions in early adolescence than in late adolescence/early adulthood, as primary myelination reaches completion.

We quantify changes in lesional MTR in a cohort of adolescents with MS imaged longitudinally from mid-adolescence to early adulthood. We hypothesize that MS lesion remyelination capacity, measured by MTR recovery, (1) decreases rapidly with age in adolescents with MS, and (2) in older adolescents, reaches a level comparable to that seen in adults with MS.

2. Material and methods

2.1. Subjects

All subjects were selected from a single site (The Hospital for Sick Children, Toronto), and all were imaged on the same 1.5 T MRI scanner. Subjects were selected from two studies: our national study of acquired demyelination in Canadian children (Banwell et al., 2011),and from a serial MRI and neurocognitive study of pediatric MS (Till et al., 2011). Subjects selected from the national Canadian study were imaged from the first attack, at 3, 6 and 12 months, and annually. Subjects enrolled in the MRI and neurocognitive study were enrolled at variable timepoints post-MS onset and were imaged two to four times, 12 months apart.

For selection for the present analysis, subjects were required (1) to have a diagnosis of relapsing–remitting MS according to the McDonald 2005 criteria (Polman et al., 2005) — the 2010 McDonald criteria were not available at the time of diagnosis for many of the patients; (2) to have serial scans with high quality MTR imaging, and for these scans to include at least one scan prior to detection of a new lesion, one scan with a new lesion, and one scan at least 6 months after the scan with the new lesion; (3) to be between 15 and 21 years of age at the time of the MRI scan with new lesions; (4) to have their new lesion scan at least 6 months after their incident attack; (5) to have all scans selected to be more than 30 days from a clinical relapse or any corticosteroid exposure; and (6) to either be free of any immunomodulatory therapy or treated with one of the current disease-modifying therapies (DMTs): glatiramer acetate (GA; Copaxone, Teva Pharmaceutical Industries, Petah Tiqva, Israel), or one of two formulations of interferon β-1a (IFN-R; subcutaneous Rebif, Merck Serono International, Geneva, Switzerland or IFN-A; intramuscular Avonex, Biogen, Cambridge, USA). No patient was treated with interferon-beta 1b so we did not include this in our criteria. Very few pediatric MS patients were exposed to other therapies, such as natalizumab or cyclophosphamide, and any such patients were excluded.

2.2. Imaging

Images were acquired on a single 1.5 T GE TwinSpeed Excite 12.0 scanner (GE Medical Systems, Milwaukee, USA). Sequences obtained included: T1-weighted (T1; sagittal SPGR, $T_R = 22$ ms, $T_E = 8$ ms, $1.5 \times 1 \times 1$ mm, flip angle 30°), T2-weighted and proton density-weighted (T2, PD; dual echo axial FSE, $T_R = 3500$ ms, $T_E = 15, 63$ ms, $1 \times 1 \times 2$ mm), and magnetization transfer images (axial SPGR, $T_R = 27$ ms, $T_E = 4$ ms, $1.5 \times 1.5 \times 1.5$ mm, flip angle 12°) with (MT_{ON}) and without (MT_{OFF}) a magnetization transfer pulse (8 ms Fermi). Voxel sizes are all right/left × anterior/posterior × superior/inferior. An adult male volunteer was also scanned at intervals on the same scanner with the same protocol as a "living phantom." MTR images were calculated for each subject at each timepoint using the formula $MTR = 100 \cdot \frac{MT_{OFF} - MT_{ON}}{MT_{OFF}}$ and normalized using the living phantom data, according to the procedure in Brown et al. (2012). This normalization process maps raw MTR measurements onto a calibrated scale, where normal white matter (WM), as defined by the living phantom, has a value of 1 and normal gray matter (GM) has a value of 0, and reduces inter-scanner variability to below the level of inter-subject variability (Brown et al., 2011), as well as corrects potential longitudinal changes in measured MTR on a single scanner. Although MTR measurements are unitless, we will refer to measurements on this scale as being in normalized MTR units (nMU) for clarity.

2.3. Preprocessing

All images for each subject were co-registered (minctracc, McConnell Brain Imaging Centre, Montreal, Quebec, Canada (Collins et al., 1994)) and probability maps for WM, GM, cerebrospinal fluid (CSF) and T2 lesions were constructed using a Bayesian classifier with the T1, T2 and PD images as input (Francis, 2004). T2 lesion masks were automatically generated from the T2 lesion probability maps, reviewed and, if necessary, edited by trained readers. Longitudinally-consistent high confidence WM and GM masks (HCWM, HCGM) were constructed, consisting of tissue identified as having greater than 85% probability WM or GM at every timepoint. Finally, *de novo* ΔMTR lesion masks were generated as previously described (Brown et al., 2012). ΔMTR lesions were segmented from MTR difference images by identifying focal areas of newly-appearing MTR signal decrease. *De novo* ΔMTR lesions were defined as those occurring in previously normal-appearing WM.

2.4. Analysis

Each lesion was assigned a unique identifier and regions of interest (ROIs) corresponding to each lesion were identified on all scans. MTR values of voxels within the ROI were averaged, producing a mean lesion MTR measurement at each timepoint. Together with the elapsed time relative to the lesion appearance, these data form an MTR timecourse for the lesion, showing MTR evolution from before lesion formation, through acute inflammation, to post-lesion follow-up. From other data (Brown et al., 2012) we have observed that MTR values in lesions change rapidly during the acute inflammatory phase, decreasing from about 1 month before the lesion is observed, recovering partially by 3 months, and then remaining relatively stable in the longer term (Brown et al., 2012). MTR measurements made during the period of acute lesion formation could be influenced by inflammation and its resolution. For these reasons, only samples acquired outside the acute period (defined as 1 month prior to 3 months after lesion formation) were included in our statistical models, although all data have been graphed to illustrate the entire timecourse.

The primary goal of the analysis was to detect changes in the amount of MTR recovery with age. However, disease duration and treatment status might be significant confounding factors. Since disease duration and age are correlated longitudinally, these should not both be factors in the same model. Therefore, we used age at onset in place of disease duration, which corrects for any effects related to disease duration, independent of the age at which a new lesion is observed.

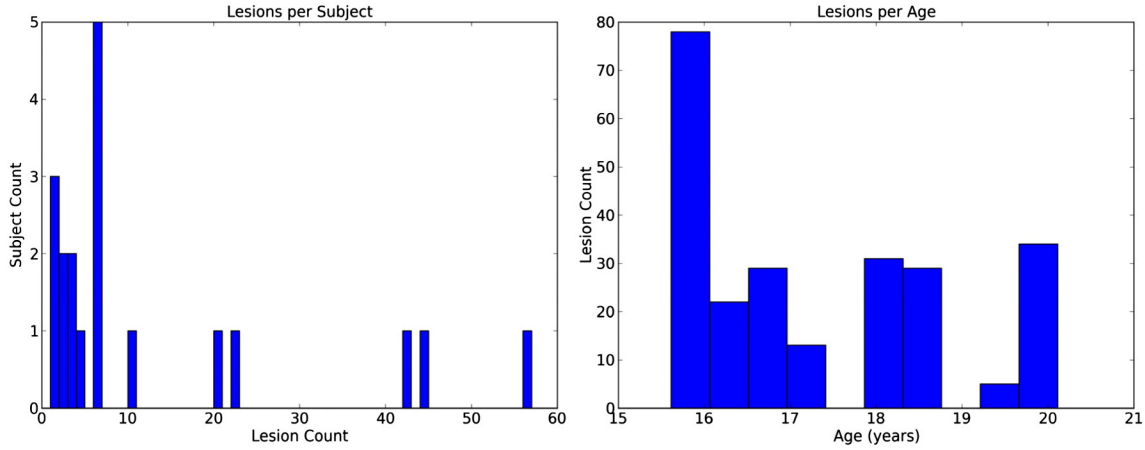

Fig. 1. Histograms of lesion distribution by subject and age. The data exhibited the expected distribution of new lesion counts with most subjects having only a few while others had many. The number of new lesions was distributed approximately uniformly by age except for an increased number around the age of 16; many subjects started disease modifying therapy around this age.

MTR timecourses were modeled using a general linear mixed model (GLMM) in R (R Team, 2010) using the lme4 package (Bates et al. 2012) with the formula:

$$MTR \sim age + ageAtOnset + treatment + recovery + recovery : age + recovery : age^2 + recovery : treatment + recovery : ageAtOnset + (1|subject/timepoint/lesion)$$

where ":" indicates an interaction and (1|subject/timepoint/lesion) is a nested random intercept. The subject's age at new lesion formation, age at onset, and treatment at the time of lesion appearance, plus a dummy variable *recovery* indicating that the MTR measurement was taken after the lesion formed, were the main fixed effects; interactions of recovery with each of age at lesion appearance, treatment, and age at onset were included. As we expected the remyelinative capacity to decrease rapidly in adolescence and then stabilize as subjects approached adulthood, we also included an interaction between age^2 and *recovery*, allowing the rate of change to accelerate or decelerate with age. The random effects were lesion, nested within timepoint, within subject. This random effects structure accounts for correlations between lesions within a subject, lesions appearing at the same timepoint, and between measurements taken over time in each lesion. The *recovery* factor measures the change in MTR from a stable pre-lesion value to stable post-lesion value. We expect the recovery to be negative, indicating that the MTR recovers only partially. The *recovery*:*age* and *recovery*:age^2 interactions measure changes in the amount of recovery demonstrated by lesions that appear in subjects at different ages. Since measurements taken from larger lesions are averaged over more voxels, these measurements have a lower variance as well as being less affected by partial volume effect. The standard error decreases by the square root of the number of averaged samples, so measurements were weighted in the model by the square root of the volume of the lesion they were taken from.

Age at lesion appearance and age at onset values were "centered" by subtracting 16 and 13, respectively, so the modeled effects are relative to a 16 year old subject with an age of onset of 13 years. Centering variables that have a non-zero mean, such as age, is a recommended modeling practice. In this case it makes explicit that a linear trend is not being imposed from birth, making interpretation of the results more straightforward. The fit of the model as a whole was evaluated by comparing the log-likelihoods of the model and a null model using a χ^2 test. If this "gateway test" was significant, individual effects were evaluated using *f*-tests, with denominator degrees of freedom estimated using a Satterthwaite approximation, by the R package MixMod (Kuznetsova and Brockhoff, 2012). This methodology eliminates the

Table 1
Subject demographics.

	Minimum	Median	Maximum
Age (years; at time of lesion appearance)	15.6	17.1	20.1
Age at First Attack (years)	5.3	13.2	16.7
Sex	Male: 2		Female: 17
Treatment (at time of lesion appearance)	No DMT: 3 IFN-A: 6		GA: 12 IFN-R: 5

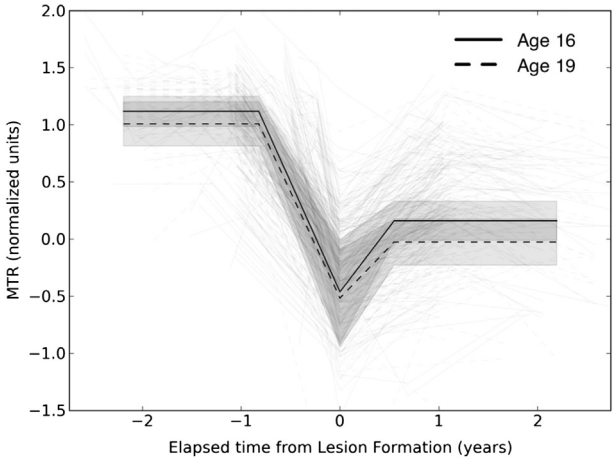

Fig. 2. MTR timecourses in *de novo* ΔMTR lesions. Light lines indicate individual timecourses while heavy lines are estimates generated from a model. Shaded areas indicate 95% confidence regions. Lesions showed MTR decreasing at the time of lesion formation (time 0), then recovering partially afterward. The *recovery* value is the difference between the stable post-lesion value and the stable pre-lesion value. Sample curves from the model for an average 16 year old (solid) and a 19 year old (dashed), both with MS onset at age 13, are shown.

Table 2
Parameter estimates of the statistical model.

Effect	Estimate (nMU)	Prediction (nMU, reference subject)	Degrees of freedom	*f*	*p*
Intercept	1.10	1.10	–	–	–
Age	−0.013/year	1.10	1/34	0.00	0.99
Recovery	**−0.65**	**0.45**	**1/480**	**263**	**<0.0001**
Recovery:age at onset	**−0.015/year**	**0.45**	**1/431**	**12.8**	**0.0004**
Recovery:age	**−0.19/year**	**0.45**	**1/518**	**5.18**	**0.023**
Recovery:age^2	0.032/year^2	0.45	1/504	0.740	0.39
Recovery:treatment (IFN-A)	**0.08**	**0.53**	**3/463**	**6.46**	**0.0003**
Recovery:treatment (IFN-R)	**0.0067**	**0.45**			
Recovery:treatment (GA)	**−0.23**	**0.22**			
Random effects	$\chi^2 = 223; p < 0.00001$				
Lesion	Variance = 0.056				
Timepoint	Variance = 0.000				
Subject	Variance = 0.040				
Residual	Variance = 0.066				

p > 0.05 using a standard general linear mixed model f-test with denominator degrees of freedom estimated by the Satterthwaite approximation, as discussed in the methods.

need for multiple comparisons when examining orthogonal contrasts within the model. R^2 values were produced according to the procedure suggested by Nakagawa and Schielzeth (2012), where the marginal R^2 is the variance explained by the fixed effects alone, and the conditional R^2 is the variance explained by the entire model including random effects.

Measurements of the post-lesion MTR value have less statistical power to detect changes in recovery than the pre- to post-lesion difference (Brown et al., 2012), but may be useful for comparisons when the pre-lesion MTR values are very different, such as when comparing subjects with short disease duration with those who have long-standing diffuse white matter changes. These values were calculated by summing the relevant factors from the model.

3. Results

The final dataset included data from 241 new lesions in 19 pediatric-onset MS patients (2 males, 17 females). Lesions were identified on 26 unique scans, thus several subjects had new lesions at more than one timepoint (Fig. 1). Subjects were aged 15.6–20.1 years (mean 17.4, median 17.1) at the time of lesion appearance and age at first attack ranged from 5.3 to 16.7 years (mean 12.5, median 13.2). Treatments at the time of lesion appearance were IFN-R: 5; IFN-A: 6; GA: 12 and no DMT: 3. Demographic data are summarized in Table 1.

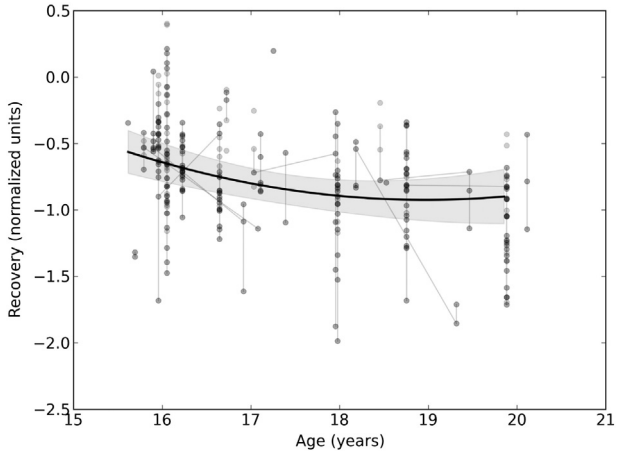

Fig. 3. The difference between post- and pre-lesion MTR by age. A recovery value of 0 indicates full post-lesion MTR recovery to baseline while negative values indicate partial recovery. Circles indicate measured values in individual lesions. Light lines connect mean values for subjects with new lesions and enough data to measure recovery at multiple timepoints. The dark line indicates the model prediction for the average subject and the shaded area is the 95% confidence region. MTR recovery decreases significantly with age.

As illustrated in Fig. 2, an acute decrease in MTR at the time of lesion formation was noted, followed by partial recovery. Table 2 provides the results of the model fit. The model fit is significantly better than the null model ($p < 0.0001$) and achieved a marginal R^2 of 0.54 and a conditional R^2 of 0.81. Pre-lesion MTR values had a mean of 1.10 nMU and did not change significantly with age at scan ($p = 0.99$). New MTR lesions exhibited a significant reduction of MTR signal to a post-lesion level of 0.65 nMU ($p < 0.0001$) in the reference case (age = 16, age at onset = 13, no DMT). Older age at onset was associated with slightly poorer recovery (−0.015 nMU/year; $p = 0.0004$). MTR signal recovery within lesions decreased significantly with increasing age at lesion appearance (−0.19 nMU/year, $p = 0.023$). The quadratic term age^2 was positive, but not significant (0.032 nMU/year^2; $p = 0.39$). Treatment with DMTs was also a significant factor in recovery ($p = 0.0003$).

Since the recovery–age relationship is of primary interest and quadratic terms can have large effects on model fits, the model was refit without the age^2 factor, yielding similar results and no change in the statistical significance of any factors. To determine whether our results were impacted by a small number of subjects with a large number of lesions, we fit the model using subject-wise data where values from lesions within individual subjects were averaged. Although *p*-values in the resulting model were increased due to the effective reduction in sample size, the model yielded similar results, with no change in significance except for the *recovery:age at onset* factor ($p = 0.34$).

Fig. 3 shows the pre- to post-lesion MTR difference (*recovery*) as a function of age at lesion appearance. The round markers indicate measurements in individual lesions. Some subjects had recovery measurements from lesions at more than one timepoint, and these are indicated by light lines joining the volume-weighted mean recovery value at each timepoint. Vertical lines connect measurements from multiple new lesions at the same timepoint in individual subjects. A predicted mean curve from the model is shown as a heavy line with shading indicating the 95% confidence region.

The *Prediction* column of Table 2 gives predicted MTR values for the reference case: the predicted post-lesion MTR value for untreated 16 year olds (onset at age 13) was 0.45 nMU while for eighteen year olds it was 0.13.

4. Discussion

We demonstrated an age-related decline in lesional recovery during adolescence and into early adulthood. The onset of MS during childhood

and adolescence is associated with limited accrual of physical disability in the first 10 years of disease (Bigi and Banwell, 2012; Boiko et al., 2002; Renoux et al., 2007, 2008; Yeh et al., 2009a). Although there may exist several explanations for the preservation of physical function seen in pediatric MS patients, one possible mechanism could be effective repair of lesions. We and others have shown that the overall lesion burden, as measured by both T2- and T1-weighted images, is similar in pediatric- and adult-onset MS (Ghassemi et al., 2008a, b; Yeh et al., 2009b). Thus, the lower risk of physical disability cannot be attributed to a lower lesion burden in children and adolescents. We have also recently shown that pediatric-onset MS patients have lower global and regional brain volumes, compared to healthy age- and sex-matched pediatric populations (Aubert-Broche et al., 2011; Kerbrat et al., 2012), further indicating that pediatric-onset MS patients are not spared from the injurious pathology that characterizes MS. Thus, preserved physical functioning in the face of active inflammatory disease may relate to improved remyelination within lesions or potentially to a heightened capacity of pediatric patients to marshal alternative neural networks (plasticity).

Although we did not have an adult control group acquired on the same scanner with the same protocol with which to compare, published data in adults (Brown et al., 2012) offers a qualitative comparator. We previously report pre-lesion MTR values in adults of about 0.5 nMU, which compares to 1.1 nMU in adolescents in this study; normal adult WM has a median value of 1.0 nMU. Children and young adolescents are expected to have slightly higher WM MTR than normal adults because MTR has been observed to decrease slightly, at least in males, during adolescence (Perrin et al., 2008). The very low pre-lesion value observed in adults with MS suggests that these patients have accumulated considerable diffuse WM damage.

Post-lesion MTR values in *de novo* ΔMTR lesions in adults were approximately 0 nMU (Brown et al., 2012), compared to 0.45 nMU and 0.13 nMU in sixteen and eighteen year olds, respectively. These values indicate that early adolescents enjoy a heightened capacity for remyelination compared to late adolescence and adulthood. Adult patients between 18 and 20 years of age were already demonstrating post-lesion MTR values comparable to those seen in older adults. This observation, as well as the positive age^2 effect estimated by our model, is consistent with the hypothesis that young adolescents enjoy a heightened capacity for remyelination, which is lost as they enter adulthood.

Reduced remyelinative capacity in late adolescence could be caused by the loss of factors uniquely associated with brain development, which are lost at the end of adolescence, or by the same processes that produce slow decline in adults. Various studies, primarily in animals, have attempted to identify the causes of adult age-related decreases in remyelination. These have observed increasing delays in (1) colonization of lesions by oligodendrocyte precursor cells (OPCs) (Sim et al., 2002), (2) OPC differentiation (Sim et al., 2002), (3) up-regulation of growth factor expression (Hinks and Franklin, 2000) and (4) macrophage response (Hinks and Franklin, 2000; Ruckh et al., 2012) with increasing age, as well as inefficient suppression of OPC differentiation inhibitors (Shen et al., 2008) and decreased efficiency of myelin debris clearance (Gilson and Blakemore, 1993). Recently, Ruckh et al. used rats with surgically connected circulatory systems (parabiotically bound partners) to demonstrate that remyelination in older rats can be improved through the availability of peripheral macrophages provided by young partners (Ruckh et al., 2012).

Associations between adolescent brain development and myelination are suggested by the observation that white matter volume increases during adolescence and early adulthood (Aubert-Broche et al., 2013; Lenroot et al., 2007; Perrin et al., 2008). This may be due to ongoing primary myelination, which might continue into early adulthood, at least in some brain regions (Benes et al., 1994; LaMantia and Rakic, 1990, 1994). There is also evidence that late adolescent growth in white matter may be at least partially due to increases in axon caliber (Perrin et al., 2008), which may require active remodeling of the myelin sheath to accommodate thickening axons. These processes may be supported by an adolescent brain microenvironment that is also more favorable for robust remyelination.

The association we observed between older age at disease onset and *poorer* recovery is at first glance surprising: later onset implies shorter disease duration for a subject of a given age. Since disease duration is correlated with both age and age at onset, it can be difficult to separate the effects of these three factors, but it is possible that patients who develop MS at a younger age may experience delayed development, retaining remyelination-enhancing developmental factors to an older age.

We detected a significant decrease in MTR recovery in lesions in adolescent MS patients imaged from mid-adolescence to early adulthood. The heightened reparative capacity in the younger adolescents may, in part, explain the limited physical disability seen in these patients. Whether the relative loss of reparative capacity in early adulthood will render patients at the same risk of disability as adult-onset MS patients remains to be seen. Further studies of even younger MS patients will determine whether myelin repair is even greater in periods of more active primary myelination.

Conflicts of interest

Dr. Arnold has served on advisory boards, received speaker honoraria, or served as a consultant for Acorda, Bayer, Biogen Idec, Eli Lilly, Serono, Genentech, Genzyme, GSK, MedImmune, Novartis, Opexa Therapeutics, Receptos, Roche, Sanofi-Aventis, and Teva. He has an ownership interest and receives income from NeuroRx Research Inc., and has received, through McGill University, research funding from Bayer Healthcare. Drs. Narayanan and Brown have received financial compensation from NeuroRx Research for consulting services. Dr. Banwell serves as a consultant for Biogen-Idec, Sanofi, and Novartis.

Acknowledgments

This work was supported by the Canadian Multiple Sclerosis Scientific Research Foundation and the Canadian Institutes of Health Research; and RAB received personal support from the Multiple Sclerosis Society of Canada.

Appendix A

Table A.1
Parameter estimates of the subject-wise statistical model.

Effect	Estimate (nMU)	Degrees of freedom	*f*	*p*
Intercept	1.18	–	–	–
Age	−0.044/year	1/22	0.97	0.33
Recovery	**−0.75**	**1/48**	**24**	**<0.0001**
Recovery:age at onset	−0.0075/year	1/66	0.91	0.34
Recovery:age	**−0.073/year**	**1/48**	**4.1**	**0.049**
Recovery:treatment (IFN-A)	**0.23**	**3/62**	**3.6**	**0.018**
Recovery:treatment (IFN-R)	**0.037**			
Recovery:treatment (GA)	**−0.041**			
Random effects				
Subject	Variance = 0.20			
Residual	Variance = 0.76			

$p < 0.05$ on a standard general linear mixed model f-test using denominator degrees of freedom estimated by a Satterthwaite approximation, as discussed in the methods.

References

Aubert-Broche, B., et al., 2013. A new method for structural volume analysis of longitudinal brain MRI data and its application in studying the growth trajectories of anatomical brain structures in childhood. Neuroimage 82, 393–402. http://dx.doi.org/10.1016/j.neuroimage.2013.05.06523719155.

Aubert-Broche, B., et al., 2011. Regional brain atrophy in children with multiple sclerosis. Neuroimage 58, 409–415. http://dx.doi.org/10.1016/j.neuroimage.2011.03.02521414412.

Banwell, B., et al., 2011. Clinical, environmental, and genetic determinants of multiple sclerosis in children with acute demyelination: a prospective national cohort study. Lancet. Neurology 10, 436–445. http://dx.doi.org/10.1016/S1474-4422(11)70045-X21459044.

Banwell, B., Ghezzi, A., Bar-Or, A., Mikaeloff, Y., Tardieu, M., 2007. Multiple sclerosis in children: clinical diagnosis, therapeutic strategies, and future directions. Lancet. Neurology 6, 887–902. http://dx.doi.org/10.1016/S1474-4422(07)70242-917884679.

Barkhof, F., et al., 2003. Remyelinated lesions in multiple sclerosis: magnetic resonance image appearance. Archives of Neurology 60, 1073–1081. http://dx.doi.org/10.1001/archneur.60.8.107312925362.

Bates, D., Maechler, M., Bolker, B., 2012. lme4: Linear Mixed-Effects Models Using S4 Classes. R Packageversion 0.999999-0.

Benes, F.M., Turtle, M., Khan, Y., Farol, P., 1994. Myelination of a key relay zone in the hippocampal formation occurs in the human brain during childhood, adolescence, and adulthood. Archives of General Psychiatry 51, 477–484. http://dx.doi.org/10.1001/archpsyc.1994.03950060041048192550.

Bigi, S., Banwell, B., 2012. Pediatric multiple sclerosis. Journal of Child Neurology 27, 1378–1383. http://dx.doi.org/10.1177/088307381245278422914372.

Boiko, A., Vorobeychik, G., Paty, D., Devonshire, V., Sadovnick, D., 2002. Early onset multiple sclerosis: a longitudinal study. Neurology 59, 1006–1010. http://dx.doi.org/10.1212/WNL.59.7.100612370453.

Brown, R.A., Narayanan, S., Arnold, D.L., 2012. Segmentation of magnetization transfer ratio lesions for longitudinal analysis of demyelination and remyelination in multiple sclerosis. Neuroimage 66C, 103–109. http://dx.doi.org/10.1016/j.neuroimage.2012.10.05923110887.

Brown, R.A., Narayanan, S., Freedman, M., Atkins, H.L., Arnold, D.L., 2011. Normalization of magnetization transfer ratio MRI for multicentre clinical trials. International Society for Magnetic Resonance in Medicine Annual Conference and Exhibition 4082.

Chen, J.T., et al., 2007. Voxel-based analysis of the evolution of magnetization transfer ratio to quantify remyelination and demyelination with histopathological validation in a multiple sclerosis lesion. Neuroimage 36, 1152–1158. http://dx.doi.org/10.1016/j.neuroimage.2007.03.07317543541.

Collins, D.L., Peters, T.M., Evans, A.C., 1994. Automated 3D nonlinear deformation procedure for determination of gross morphometric variability in human brain. Proceedings of S.P.I.E. 2359, 180. http://dx.doi.org/10.1117/12.185178.

Deloire-Grassin, M.S.A., et al., 2000. In vivo evaluation of remyelination in rat brain by magnetization transfer imaging. Journal of the Neurological Sciences 178, 10–16. http://dx.doi.org/10.1016/S0022-510X(00)00331-211018243.

Dousset, V., et al., 1992. Experimental allergic encephalomyelitis and multiple sclerosis: lesion characterization with magnetization transfer imaging. Radiology 182, 483–491. http://dx.doi.org/10.1148/radiology.182.2.17329681732968.

Fancy, S.P.J., et al., 2010. Overcoming remyelination failure in multiple sclerosis and other myelin disorders. Experimental Neurology 225, 18–23. http://dx.doi.org/10.1016/j.expneurol.2009.12.02020044992.

Francis, S.J., 2004. PhD Thesis Automatic Lesion Identification in MRI of Multiple Sclerosis Patients.

Franklin, R.J.M., Zhao, C., Sim, F.J., 2002. Ageing and CNS remyelination. Neuroreport 13, 923–928. http://dx.doi.org/10.1097/00001756-200205240-0000112004191.

Ghassemi, R., et al., 2008a. Quantitative comparison of regional lesion burden between children and adults with clinically definite multiple sclerosis. 60th Annual Meeting of the American Academy of Neurology 70, 12–19.

Ghassemi, R., et al., 2008b. Lesion distribution in children with clinically isolated syndromes. Annals of Neurology 63, 401–405. http://dx.doi.org/10.1002/ana.2132218306242.

Gilson, J., Blakemore, W.F., 1993. Failure of remyelination in areas of demyelination produced in the spinal cord of old rats. Neuropathology and Applied Neurobiology 19, 173–181. http://dx.doi.org/10.1111/j.1365-2990.1993.tb00424.x8316337.

Hinks, G.L., Franklin, R.J.M., 2000. Delayed changes in growth factor gene expression during slow remyelination in the CNS of aged rats. Molecular and Cellular Neurosciences 16, 542–556. http://dx.doi.org/10.1006/mcne.2000.089711083917.

Kerbrat, A., et al., 2012. Reduced head and brain size for age and disproportionately smaller thalami in child-onset MS. Neurology 78, 194–201. http://dx.doi.org/10.1212/WNL.0b013e318240799a22218275.

Kuznetsova, A., Brockhoff, P.B., 2012. MixMod: Analysis of Mixed Models. R Packageversion 1.

LaMantia, A.S., Rakic, P., 1994. Axon overproduction and elimination in the anterior commissure of the developing rhesus monkey. Journal of Comparative Neurology 340, 328–336. http://dx.doi.org/10.1002/cne.9034003048188854.

LaMantia, A.S., Rakic, P., 1990. Axon overproduction and elimination in the corpus callosum of the developing rhesus monkey. Journal of Neuroscience: the Official Journal of the Society for Neuroscience 10, 2156–21752376772.

Lenroot, R.K., et al., 2007. Sexual dimorphism of brain developmental trajectories during childhood and adolescence. Neuroimage 36, 1065–1073. http://dx.doi.org/10.1016/j.neuroimage.2007.03.05317513132.

Miller, D.J., Asakura, K., Rodriguez, M., 1996. Central nervous system remyelination clinical application of basic neuroscience principles. Brain Pathology (Zurich, Switzerland) 6, 331–344. http://dx.doi.org/10.1111/j.1750-3639.1996.tb00859.x8864288.

Nakagawa, S., Schielzeth, H., 2012. A general and simple method for obtaining R2 from generalized linear mixed-effects models. Methods in Ecology and Evolution.

Patrikios, P., et al., 2006. Remyelination is extensive in a subset of multiple sclerosis patients. Brain: A Journal of Neurology 129, 3165–3172. http://dx.doi.org/10.1093/brain/awl21716921173.

Perrin, J.S., et al., 2008. Growth of white matter in the adolescent brain: role of testosterone and androgen receptor. Journal of Neuroscience: the Official Journal of the Society for Neuroscience 28, 9519–9524. http://dx.doi.org/10.1523/JNEUROSCI.1212-08.200818799683.

Pike, G.B., et al., 2000. Multiple sclerosis: magnetization transfer MR imaging of white matter before lesion appearance on T2-weighted images. Radiology 215, 824–830. http://dx.doi.org/10.1148/radiology.215.3.r00jn0282410831705.

Polman, C.H., et al., 2005. Diagnostic criteria for multiple sclerosis: 2005 revisions to the "McDonald Criteria". Annals of Neurology 58, 840–846. http://dx.doi.org/10.1002/ana.2070316283615.

R Team, 2010. R: A Language and Environment for Statistical Computing. R Foundation for Statistical Computing, Vienna, Austria.

Renoux, C., Vukusic, S., Confavreux, C., 2008. The natural history of multiple sclerosis with childhood onset. Clinical Neurology and Neurosurgery 110, 897–904. http://dx.doi.org/10.1016/j.clineuro.2008.04.00918534742.

Renoux, C., et al., 2007. Natural history of multiple sclerosis with childhood onset. New England Journal of Medicine 356, 2603–2613. http://dx.doi.org/10.1056/NEJMoa06759717582070.

Ruckh, J.M., et al., 2012. Rejuvenation of regeneration in the aging central nervous system. Cell Stem Cell 10, 96–103. http://dx.doi.org/10.1016/j.stem.2011.11.01922226359.

Ruggieri, M., Iannetti, P., Polizzi, A., Pavone, L., Grimaldi, L.M.E., 2004. Multiple sclerosis in children under 10 years of age. Neurological Sciences: Official Journal of the Italian Neurological Society and of the Italian Society of Clinical Neurophysiology 25 (Suppl 4), S326–S335. http://dx.doi.org/10.1007/s10072-004-0335-z15727227.

Schmierer, K., Scaravilli, F., Altmann, D.R., Barker, G.J., Miller, D.H., 2004. Magnetization transfer ratio and myelin in postmortem multiple sclerosis brain. Annals of Neurology 56, 407–415. http://dx.doi.org/10.1002/ana.2020215349868.

Shen, S., et al., 2008. Age-dependent epigenetic control of differentiation inhibitors is critical for remyelination efficiency. Nature Neuroscience 11, 1024–1034. http://dx.doi.org/10.1038/nn.217219160500.

Sim, F.J., Zhao, C., Penderis, J., Franklin, R.J.M., 2002. The age-related decrease in CNS remyelination efficiency is attributable to an impairment of both oligodendrocyte progenitor recruitment and differentiation. Journal of Neuroscience: the Official Journal of the Society for Neuroscience 22, 2451–245920026217.

Till, C., et al., 2011. MRI correlates of cognitive impairment in childhood-onset multiple sclerosis. Neuropsychology 25, 319–332. http://dx.doi.org/10.1037/a002205121534686.

Yeh, E.A., et al., 2009a. Pediatric multiple sclerosis. Nature Reviews. Neurology 5, 621–631. http://dx.doi.org/10.1038/nrneurol.2009.15819826402.

Yeh, E.A., et al., 2009b. Magnetic resonance imaging characteristics of children and adults with paediatric-onset multiple sclerosis. Brain: A Journal of Neurology 132, 3392–3400. http://dx.doi.org/10.1093/brain/awp27819892770.